Adiabatic hypercooling of binary melts

Kirk Brattkus
Department of Mathematics, Southern Methodist University, Dallas, Texas 75275-0156
(Received 22 November 1999)

A binary melt is hypercooled when it is cooled to a temperature below its solidus. In the isothermal limit planar solidification fronts propagate at a constant velocity determined by the kinetic undercooling and are subject to a long-wavelength morphological instability if speeds fall below a critical value. Here we examine the adiabatic limit where the accumulation of a small latent heat release causes the velocity of the interface to slowly decrease through its critical value. The evolution of the hypercooled interface is governed by a damped Kuramoto-Sivashinsky (dKS) equation with coefficients that vary as the interface decelerates. Using this equation we show that morphological transitions are delayed by an amount that reflects both the time the system spends in a stable state and the magnitude of the damping. For a sufficiently large latent heat of fusion the long-wavelength morphological instability is annihilated. Finally, the adiabatic dKS equation predicts late-stage coarsening of the microstructure with length scales that increase as $t^{1/2}$. In finite systems this coarsening removes the morphological instability.

PACS number(s): 81.10.Aj, 81.10.Fq, 81.30.Fb

Morphology is less likely to develop on microscopically rough interfaces during rapid solidification because of the enhanced effects of surface energy. As solidification velocities increase, the thickness of the diffusive boundary layer ahead of the front decreases, and this results in a corresponding decrease in the length scales of the interfacial morphology. Since small interfacial scales are energetically unfavorable, there are often limits of absolute stability where planar solidification fronts that are unstable at low growth rates are restabilized at large growth rates. Two examples of such an absolute stability limit occur for the Mullins-Sekerka instability in directionally solidified binary melts [1] and in hypercooled pure melts [2]. The transitions near both of these absolute stability limits occur at wavelengths that are large in comparison to the thickness of the boundary layer and long-wavelength evolution equations may be derived that describe the transition [2–6].

These regimes are difficult to access experimentally. A restabilization at large velocity has been observed in experiments on liquid crystals with an isotropic-nematic transition that mimics the directional solidification of a binary melt [7]. Hypercooled pure melts have also been observed [8] but the growth rates at which the planar fronts restabilize occur at unattainably large undercoolings. Absolutely stable hypercooled fronts have apparently only been observed for the superfluid ^{3}He *A-B* phase transition [9] where extremely large surface energies preclude homogeneous nucleation.

Hypercooling occurs when microscopic attachment kinetics at the interface limits the velocity of the front to such an extent that the rate limiting species may be diffused away fast enough to allow fronts which propagate at constant velocity. Although hypercooling is difficult to achieve in pure melts, it has been argued [3] that it should be easily achievable in binary melts where hypercooling occurs when undercoolings are set below the equilibrium solidus. In fact, experiments on such constitutionally hypercooled binary alloys have been performed using the transparent plastic crystal succinonitrile and salol [10]. Experimental observations are reported of unexpected microstructures in the hypercooled region but the investigators were unaware of the criterion for absolute stability and do not report on having observed stable planar fronts. Nonisothermal effects were clearly present in these experiments and all existing theories of hypercooled binary melts are isothermal.

We begin by considering a uniform liquid melt at an initial concentration C_i and temperature T_i. The melt will remain in equilibrium as long as T_i is greater than the temperature at its liquidus, $T_l = T_M + mC_i$. Here T_M is the melting temperature of a pure substance and m is the slope of the liquidus linearized for small solute concentrations. If T_i falls below T_l, the liquid is undercooled and it will solidify. Due to segregation, the concentration in the liquid just ahead of the solidification front will quickly rise to C_i/k where $k < 1$ is the segregation coefficient and form a miscibility gap at the interface of $\Delta C = (1-k)C_i/k$. If we define the degree of undercooling to be $\Delta = (T_i - T_l)/m\Delta C$, then the liquid is hypercooled to a temperature below the temperature at its equilibrium solidus, $T_s = T_l + m\Delta C$, when $\Delta > 1$.

If the latent heat of fusion per unit volume L_v is zero, the solidification will proceed isothermally at a rate that is controlled by the solute diffusivity D. The isothermal solidification of a binary alloy is analogous to the solidification of a pure melt and, in fact, the governing equations are identical if the miscibility gaps are constant. By analogy then it is immediately clear that there are three distinct long-time behaviors for the velocity v of a planar front solution depending on the size of the undercooling. For $0 < \Delta < 1$ the system is undercooled and $v = O(t^{-1/2})$ as $t \to \infty$; for $\Delta = 1$ the system is on the border between being undercooled and hypercooled and $v = O(t^{-1/3})$ as $t \to \infty$; for $\Delta > 1$ the system is hypercooled and $v = O(1)$ as $t \to \infty$ [11].

Undercooled and hypercooled growth are subject to a Mullins-Sekerka instability [12] below the limit of absolute stability $\Delta < \Delta_c = 1 + (\gamma k)^{-1}$ where the parameter $\gamma = \beta T_m d_0/D$ is defined here in terms of the capillary length d_0 and the coefficient of interface attachment kinetics, β. At larger hypercoolings $\Delta > \Delta_c$, planar solidification fronts are

linearly stable [3]. As Δ decreases through Δ_c, a long-wavelength instability occurs [2–4] and the development of the transition is governed by the Kuramoto-Sivashinsky (KS) equation [13].

In a coordinate system translating with velocity v the diffusion equation for u, the deviation of the solute concentration from its initial value C_i scaled on the miscibility gap ΔC, is

$$u_t = \nabla^2 u + v u_z . \tag{1}$$

The conservation of mass at an interface $z=h$ moving at a normal velocity v_n (measured in the stationary frame) with curvature $\mathcal{K}$ requires that $\nabla_n u + v_n[k+(1-k)u]=0$. The condition of thermodynamic equilibrium at the interface further requires $u=\Delta - v_n - \gamma\mathcal{K} - \lambda\theta$ where $\lambda = DL_v/k_T|m|\Delta C$ is the latent heat made nondimensional in combination with the thermal conductivity k_T and θ is the deviation of the temperature at the interface from its initial value T_i scaled by DL_v/k_T. Lengths have been scaled on the kinetic length, D/β, and time has been scaled on the diffusive time, D/β^2.

When the latent heat is zero and the liquid is hypercooled, the solidification is isothermal and planar fronts propagate at a constant velocity $v=\Delta-1$. When latent heat is not identically zero, the solidification will not remain isothermal. However, when the latent heat is small the system will undergo an adiabatic change in temperature that produces a slow modification in the solidification velocities that can be determined. To do this we first assume that since thermal diffusivities for metal alloys are typically three to four orders of magnitude larger than the mass diffusivities which control the solidification rate, the temperature fields are quasistatic. If the temperature is fixed to be T_i along a bounding wall where the liquid first freezes, then the nondimensional temperature at the interface at time t for a thermally symmetric model is

$$\theta = v\int_0^t v. \tag{2}$$

The effect of latent heat remains small unless, over time, the term $\lambda\theta$ in the condition of thermodynamic equilibrium becomes significant. After diffusive transients have decayed the concentration adopts an exponential profile $u=\exp(-vz)$, and we assume that times are so large that the integral term in the equation defining θ is significant. An ordered expansion in λ may then be developed under the assumption that $\lambda t = O(1)$ and it is found that to leading order the velocity of the planar front is given by

$$v = \frac{v_i}{\sqrt{1+2\lambda v_i t}} \tag{3}$$

where the initial velocity is $v_i=\Delta-1$. Although for very long times a hypercooled binary melt that releases a small amount of latent heat as it solidifies behaves as if it were undercooled with $v=O(t^{-1/2})$ as $\lambda t\to\infty$, hypercooled growth is distinguished from undercooled growth by the path the solidification process traces out in the equilibrium phase diagram. For hypercooled growth the concentration at the interface remains at a nearly constant value C_i/k while the temperature at the interface increases monotonically to the value T_s. For undercooled growth the term $\lambda\theta$ remains uniformly small for all time and nonzero latent heat acts as a regular perturbation to the isothermal problem. The interfacial temperature of the undercooled melt remains nearly constant at the value T_i while the concentration at the interface increases to the value $C_i+(T_i-T_l)/m$. Hypercooled melts trace out vertical paths in the phase diagram while undercooled melts trace out horizontal paths.

The transition near the absolute stability limit for an isothermally hypercooled binary melt occurs at zero wave numbers and the nonlinear dynamics is described by a long-wavelength evolution equation [14]. For velocities just below the critical velocity $v_c=\Delta_c-1$ the long-wavelength modes are linearly unstable and the nonlinear development of the transition is governed by the KS equation [3]. This picture is modified in three ways when the latent heat is small but nonzero. First, the latent heat causes the interface to slowly decelerate so that the coefficients of the corresponding KS equation are slowly varying functions of time. If the initial velocity v_i is larger than v_c, there is a slow passage through the long-wavelength instability. Second, the latent-heat release produces temperature gradients at the front which stabilize the interface. This stabilization appears as a linear damping term in the KS equation [15,16]. And third, the temperature field near the nonplanar front is a nonlocal function of the interface displacement [17,18] which appears as a nonlocal contribution to the KS equation. In our case, if the translation of the coordinate system is chosen so that the interface has zero mean, these nonlocal terms are also nonlinear. If we exclude these nonlinear nonlocal terms, then the corresponding damped Kuramoto-Sivashinsky (dKS) equation with time-dependent coefficients that models the long-wave transition near absolute stability for adiabatically hypercooled binary melts is

$$\partial_t h + \frac{v_c - v}{k v_c v}\,\partial_x^2 h + \frac{k v_c + v}{k^2 v_c v^3}\,\partial_x^4 h + \frac{1}{2k}(\partial_x h)_0^2 + \lambda v h = 0, \tag{4}$$

where the symbol $(\partial_x h)_0^2$ represents the nonlinear term less its mean value. As λ tends toward zero the velocity tends toward the constant v_i and the adiabatic dKS equation becomes the KS equation governing isothermal growth. The time-dependent coefficients in the adiabatic dKS equation for nearly hypercooled binary alloys are reminiscent of the KS equation derived for spherically expanding flames [19]. The derivation of the equation requires that the length scales which describe the morphology along the front be large in comparison to v^{-1}, the thickness of the solutal boundary layer ahead of the front.

The long-wavelength evolution equation allows us to simply examine the linear stability of the planar front which represents a time-dependent basic-state solution to the solidification problem. Often it is difficult to decide on what is meant by the stability of a time-dependent base state but, within the contexts of the evolution equation, the issue of stability can be made clear. We define the planar front solution to be linearly stable if the amplitudes of all Fourier

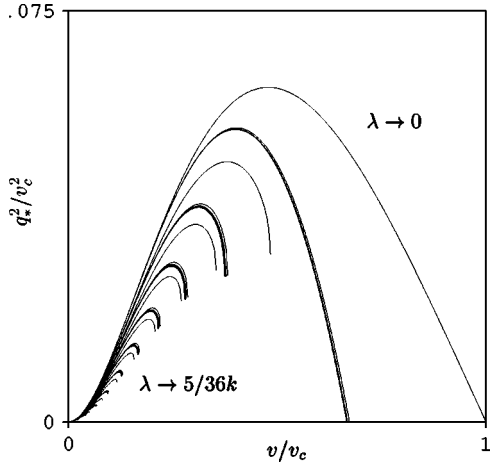

FIG. 1. The scaled wave number cutoff q_* vs the interface velocity v for $k=1/2$. At each value of the latent-heat parameter, $0<\lambda<5/36k$, there is a family of curves for $1<v_i/v_c<50$. The bold curves are the asymptotes for each family as $v_i/v_c \to \infty$.

coefficients, $\hat{h}(q,t)$, for solutions to the linearized evolution equation are smaller than their initial values. If at any point in time the power spectrum is no longer bounded by the initial spectrum, the solution is said to be unstable. Although this is a rather strong restriction which ignores the possibility of transient growth and eventual relaxation [20], it appears to give a sensible indication of when sustained growth begins to occur in numerical simulations of the adiabatic dKS equation.

The Fourier coefficients of the linearized equation (4) normalized by their initial values satisfy

$$\ln\left|\frac{\hat{h}(q,t)}{\hat{h}(q,0)}\right| = 1 - \frac{v_i}{v} + \left[\frac{(v_i^3 - v^3)}{3k\lambda v_i^2 v^3} - \frac{(v_i^2 - v^2)}{2k\lambda v_i v_c v^2}\right] q^2 - \left[\frac{(v_i^5 - v^5)}{5k\lambda v_i^4 v^5} + \frac{(v_i^4 - v^4)}{4k^2 \lambda v_i^3 v_c v^4}\right] q^4. \tag{5}$$

When v slowly decreases from $v_i > v_c$ the planar front is initially stable and amplitudes relax to zero exponentially fast. In the absence of noise, the Fourier coefficients decrease substantially in this initially stable period. In fact, the solution remains stable as the instantaneous velocity v passes through the critical value v_c. The spectrum experiences its first growth at a delayed transition velocity v_d which is well approximated for λ not too small by

$$(5 - 36\lambda k) v_d^{-1} = 5\left(3 + \frac{5}{4k}\right) v_c^{-1} - 36\lambda k v_i^{-1}. \tag{6}$$

The larger the values of λ and v_i, the smaller the values of v_d and the longer the delay in the development of the instability. As λ approaches a critical value $5/36k$, the delayed velocity tends toward zero which takes an infinite time to achieve. For larger values of the latent-heat parameter, planar fronts remain stable.

When $0<\lambda<5/36k$ an instability occurs for $v<v_d$. Latent heat has stabilized the zero-wave-number mode and the transition occurs at a nonzero wave number. As time evolves

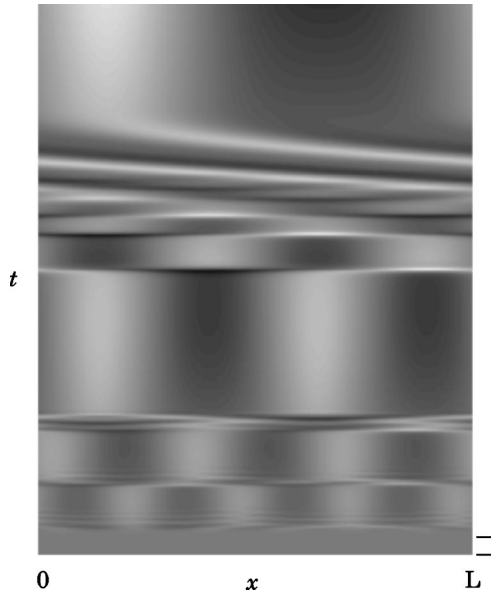

FIG. 2. A visualization of the numerical solution to Eq. (4) that uses greyscale to denote amplitude. Here the length of the interval is $L=75$, $\lambda=0.1$, and $k=1/2$. Initial conditions quickly relax to zero amplitude for $v_i=2>v_c=1$ and amplitudes remain nearly zero as velocities decrease through v_c (first mark). A delayed instability develops as velocities decrease further through the value v_d (second mark) predicted by Eq. (6). A cascade of cellular states results as the system coarsens, finally returning to a planar front (not shown). No instability is observed for $\lambda>5/36k$. Time runs from 0 to 50 units in the figure.

and v decreases below v_d, the instability develops for an interval of wave numbers bounded above by a cutoff wave number q_*. Figure 1 depicts this cutoff wave number for $k=1/2$ as a function of the velocity scaled on the critical velocity v_c. There are ten families of curves for values of λ ranging from $\lambda=0$ to $\lambda=5/36k$. Each family is composed of curves for values of the scaled initial velocity v_i/v_c ranging from $v_i/v_c=1$ to $v_i/v_c=50$. These asymptote to the thickened lines as the initial velocities become large. For $\lambda \to 5/36k$ the families collapse into the origin.

Several features of the instability are clear from this figure. First, due to the delay, the curves begin at a value of $v/v_c<1$ where the value of q_* represents the wave number of the first unstable mode. As time increases and the interface continues to decelerate, the cutoff wave number increases as the band of linearly unstable wave numbers broadens. The band continues to broaden and the length scales of the unstable modes continue to decrease until at some point in time a maximum value is reached after which the cutoff wave number begins to decrease. The structure begins to coarsen as the length scales of the linearly unstable modes increase. As velocities decrease to zero, the cutoff wave numbers scale on the velocity and, within the contexts of the linear theory, the late-stage coarsening is characterized by length scales which increase as $t^{1/2}$.

This coarsening is linked directly to the deceleration in the interface and the associated thickening of the diffusive boundary layer ahead of it. If we compare the cutoff wavelength $2\pi/q_*$ to the thickness of the diffusive boundary layer v^{-1}, we find that this ratio increases monotonically as

time evolves but is bounded above for all values of the physical parameters by a small constant slightly less than 0.2. The asymptotic derivation of the long-wavelength evolution equation is predicated on this ratio being small. Although we can control the size of this ratio only in the limit as λ tends to zero and for velocities near the critical velocity, the fact that it stays uniformly small suggests that Eq. (4) may well model the dynamics of the transition outside of this asymptotically controlled regime.

The development of the instability may be followed by numerically computing solutions to the adiabatic dKS equation. We assume periodic boundary conditions on a spatial interval of length L, apply a pseudospectral method with uniformly spaced collocation points, and integrate the coefficients of the spectral decomposition in time using VODE, a software package designed for solving stiff systems of ordinary differential equations [21].

The interface velocities are slowly varying for small values of the latent heat parameter and solutions to Eq. (4) may be interpreted as solutions to the isothermal KS equation with coefficients that are parametrized on time. For large domain sizes L, however, the interface velocities do not vary slowly on the diffusive time scale L^2t. Adiabatic variations in the speed of a solidification front will generally influence the long-time dynamics in extended systems.

A typical numerical solution to Eq. (4) for a reasonably large system $L=75$ is featured in Fig. 2. The value of the latent-heat parameter is significant here, $\lambda=0.1$, and the delay in the instability is well predicted by the velocity v_d from Eq. (6). The complicated dynamics of the KS equation reflecting spatiotemporal chaos settles down to well-defined cellular states. As velocities decrease, the system coarsens. Cells do not merge during this coarsening process; cells are lost at temporal defects that are reminiscent of phase turbulence. The persistence times for the cellular states increase as the cutoff wave number slows its approach to zero. The dynamics of the cell-cell transitions also simplifies as time evolves, for the transitions between two-cell and one-cell states heteroclinic connections and traveling waves are clearly observed. At still later times there is a transition back to a planar front.

In summary, the accumulation of latent heat in hypercooled binary melts causes solidification fronts to decelerate. We have found that absolutely stable fronts will decelerate through a delayed long-wavelength instability modeled by a damped Kuramoto-Sivashinsky equation with time-dependent coefficients and the resulting morphological instability will coarsen as velocities continue to decrease. When a latent-heat parameter is large enough the instability is annihilated.

The author would like to thank Stephen Davis for his hospitality during a recent visit to the Department of Engineering Sciences and Applied Mathematics at Northwestern University where this work was completed and to acknowledge the partial support of NSF Grant No. DMS9705089.

[1] W. Mullins and R. F. Sekerka, J. Appl. Phys. **35**, 444 (1964).
[2] M. L. Frankel, Physica D **27**, 260 (1987).
[3] C. Misbah, H. Müller-Krumbhaar, and D. E. Temkin, J. Phys. I **1**, 585 (1991).
[4] A. Umantsev and S. H. Davis, Phys. Rev. A **45**, 7195 (1992).
[5] D. C. Sarocka and A. J. Bernoff, Physica D **85**, 348 (1995).
[6] K. Brattkus and S. H. Davis, Phys. Rev. B **38**, 11 452 (1988).
[7] A. J. Simon and A. Libchaber, Phys. Rev. A **41**, 7090 (1990).
[8] M. E. Glicksman and R. J. Schaeffer, J. Cryst. Growth **1**, 297 (1967).
[9] S. T. P. Boyd and G. W. Swift, J. Low Temp. Phys. **87**, 35 (1992).
[10] O. P. Fedorov, A. G. Borisov, and V. V. Maslov, Kristallografiya **35**, 475 (1990) [Sov. Phys. Crystallogr. **35**, 274 (1990)].
[11] A. Umantsev, Kristallografiya **30**, 153 (1985) [Sov. Phys. Crystallogr. **30**, 87 (1985)].
[12] W. Mullins and R. F. Sekerka, J. Appl. Phys. **34**, 323 (1963).
[13] Y. Kuramoto, Suppl. Prog. Theor. Phys. **64**, 346 (1978); G. Sivashinsky, Acta Astronaut. **4**, 1177 (1977).
[14] M. C. Cross and P. C. Hohenberg, Rev. Mod. Phys. **65**, 851 (1993).
[15] A. Novick-Cohen, Physica D **26**, 403 (1987).
[16] K. R. Elder, J. D. Gunton, and N. Goldenfeld, Phys. Rev. E **56**, 1631 (1997).
[17] A. Novick-Cohen and G. I. Sivashinsky, Physica D **20**, 237 (1986).
[18] M. L. Frankel, Phys. Fluids A **2**, 1879 (1990).
[19] G. Sivashinsky, Acta Astronaut. **6**, 569 (1979).
[20] S. H. Davis, Annu. Rev. Fluid Mech. **30**, 87 (1976).
[21] P. N. Brown, G. D. Byrne, and A. C. Hindmarsh, SIAM (Soc. Ind. Appl. Math.) J. Sci. Stat. Comput. **10**, 1038 (1989).